rGO-ZnO nanowire deposited filamentous seaweed nanofibrous cellulose for paper supercapacitor

Priyank . L. Bhutiya (bhutiyapriyank@gmail.com)
GERMI
Rahul Kapdaia
GERMI
Brijesh Tripathi
Pandit Deendayal Energy University
Yash Sanjaliya
Pandit Deendayal Energy University
M. Abdul Rasheed
GERMI
P. L.S. Rao
GERMI
S. Zaheer Hasan
GERMI

Research Article

Keywords: Paper supercapacitor, Chaetomorpha antennina, seaweed cellulose, rGO-ZnO, Biodegradable

Posted Date: February 7th, 2023

DOI: https://doi.org/10.21203/rs.3.rs-2519176/v1

Abstract

Nanosized architectural (A Spider's web) structure of cellulose (I_α) was extracted from green seaweed *Chaetomorpha antennina* by using bleaching treatment. Further, reduced graphene oxide (rGO) and zinc oxide (ZnO) nanowire deposited over seaweed cellulose by using simple hydrothermal method. Simple press method was used to prepare rGO-ZnO seaweed cellulose nanocomposite for paper supercapacitor. This rGO-ZnO seaweed cellulose paper anode material was characterized by using various analytical techniques such as FT-IR, SEM, TGA, XRD and tensile test. XRD peaks reveals that when graphene oxide powder mixed with seaweed cellulose, it was reduced and gave Xrd peak of reduced Graphene oxide (rGO). This paper supercapacitors were tested in CV, GCD and EIS. From GCD, the specific energy density of ZnO- cellulose paper device is found to be 0.00066 Wh/kg whereas, for rGO-ZnO cellulose paper device have greater energy density of 5.21 Wh/kg. From EIS, the series resistance of ZnO- cellulose is found to be 326 Ω and for ZnO-rGO -cellulose is 2.16 Ω. This marine resources based rGO-ZnO seaweed cellulose paper supercapacitor have application in various energy storage domains including electric vehicles and electronic industries because it is bio-degradable, cost effective, thinnest, safe to use as well as high performance.

1. Introduction

For the past decades, the seaweeds have gained substantial attention all over the globe owing to their potential applications in biofuels, chemicals, hydrocolloids, cosmetics, feed, food supplements, pharmaceuticals etc. Therefore, seaweeds are harvested commercially in many parts of world because they do not need any land for farming either fertilizer or other supplements. On one side, their production

cost is very low and on the other side have high commercial market USD 11.8 billion (Sultana et al., 2022). Seaweed is a macroalgae which is found in coastal area which is attached with rock or other substrata. It is classified according to its pigmentation such as Chlorophyta (green), Rhodophyta (red) and Phaeophyta (brown). Among them Chlorophyta (green) have much more potential components in its cell wall such as carbohydrates, lipids, proteins as well as bioactive compounds. Green seaweed *Chetomorpha antennina* which is classified as filamentous algae grows on rocks with filamentous erect and reaches upto 10 cm tall in shape. It has high amount of I_{α} cellulose in its cell wall naturally (Siddhanta et al. 2011 & Bhutiya et al., 2018).

Cellulose is a linear homogeneous polysaccharide which consisting of repeated units of D-glucopyranose linked by β- 1,4 linkage. It is found in plant, algae, fungi, bacteria etc. Cellulose has drawn much attention among the researchers due to its low cost and weight, nontoxic nature, high mechanical strength, low thermal expansion, superior biodegradability and high crystallinity (Missoum, et al., 2013). Generally, it can be prepared by using harsh chemicals, enzymatic hydrolysis or mechanical treatment from lignocellulosic biomass such as wood, cotton, hemp etc. wherein, process may affect the cellulose structure as well as environment (Moon et al., 2011). Seaweed cellulose consists only d- glucose monomers as well as same X-ray diffraction (XRD) pattern from native cellulose derived from land sources. Especially, green filamentous algae such as *Chaetomorpha* or *Cladophora* consists of native nanosized cellulose -I in its cell wall naturally (Mihranyan et al., 2011). Generally, cellulose derived from wood consists I_{β} and it can be converted nanofibers I_{α} by using harsh treatment. Filamentous seaweed have I_{α} cellulose in its cell wall which have high crystallinity naturally so when it is bonded with metal oxide such as copper, zinc, silver etc. then it can be used as drug carrier, filtration media, antibacterial membrane or electrical insulator purpose [Gustafsson et al., 2016 & Bhutiya et al., 2020). Recently, seaweed derived components have been used for energy storage applications (Jiang et al., 2021 & Durairaj et al., 2022).

It is the need of time to develop the technology which is flexible, light weight or cost effective as well as biodegradable energy storage device. For this purpose, cellulose is most suitable biopolymer material for manufacturing paper based electrode material for paper supercapacitor or battery for energy storage application. Cellulose itself an insulating material that require to be coated with conductive material to make paper based energy storage device. Supercapacitor is an electrochemical charge storage device which have fast charging/ discharging cycle, high power density and longer lifecycle. Supercapacitors can be used in electronics, memory back-up system, industries, heavy machines, electric vehicles etc. It is an electrochemical double layer capacitor which can fill-up the gap between capacitors and batteries for high energy density and high power density needs. Still it have low energy density so it is difficult to replace battery. Therefore, continuous efforts are being made by researchers to increases specific capacitance. Anodic electrode material such as carbon nanotubes, graphene oxide, metal oxides, metal deposited cellulose etc. have been promising nanocomposite materials for supercapacitor applications (Jose et al., 2019). Reduced graphene oxide (rGO) with transition metal oxides such as aluminum, zinc, manganese, lithium, copper etc. have high conductivity as well as high energy density (Tafete et al.,

2022). There are many tested materials have been reported for metal oxides- cellulose nanocomposites have been tested for supercapacitor applications (Wang et al., 2017). Among these, cellulose- ZnO nanoparticles based nanocomposites have been reported recently for supercapacitor applications (Rabani et al., 2021). But only ZnO can not give good performance but when added with other transition metal oxides or polypyrrole, polyaniline or graphene oxide can provide superior performance of super capacitor (Hussain, et al., 2020 & Abdah et al., 2020). rGO-Polypyrrole- cellulose nanocomposite have been reported by Wan et al. for supercapacitor application (Wan et al., 2017). They reported that the energy density of nanocomposite was 1.18 mWh cm^{-3} by using three electrode system and also polypyrrole decreases cellulose tensile strength. Algae cellulose-metal organic framework based materials have also been reported for supercapacitor application (Zhou et al., 2019). Cotton cloth-graphene oxide (GO) has also been reported for supercapacitor applications (Etana et al., 2020). Carbon nanotubes-MnO_2 have also been reported for supercapacitor that have high energy density (16.7 kW/kg) (Wang et al., 2016). Graphene oxide-ZnO powder nanocomposites also reported for supercapacitor applications and its specific capacitance was 122.4 F/g (Saranya et al., 2016).

In present study, thread type nano fibrillated cellulose (I_α) was extracted from green filamentous seaweed *Chaetomorpha antennina* through simple bleaching process. Further, rGO-ZnO nanowires were grown over the sheet by using single step hydrothermal method and this prepared sheet can be used as anode material in paper supercapacitor. The developed electrode is used in an asymmetrical supercapacitor by sandwiching NaCl electrolyte soaked paper separator between the rGO-ZnO-seaweed cellulose nanocomposite and activated charcoal powder slurry coated nickel foil. This cost-effective, lightweight, ecofriendly seaweed based paper supercapacitor can have excellent super capacitive behavior.

2. Materials And Method

Sodium chlorite, hydrochloric acid, sodium hydroxide, sodium chloride, potassium hydroxide, and sodium carbonate were purchased from Merck, Germany. Zinc chloride was purchased from Sigma Aldrich and Graphene Oxide was purchased from Shilpa Enterprise, Nagpur, India.

2.1 Collection of Seaweed

Chaetomorpha antennina was collected from Kucchadi, (21°40'17.8"N 69°32'35"E), Porbandar, Gujarat, India in May, 2022. The seaweed was first washed with tap water to remove salts and other contaminants on it and further it was washed with distilled water and then oven dried at 50 ºC. After oven dry, seaweed was powdered using mortar and pestle.

2.2 Extraction of nanofibreous Cellulose from Seaweed

20 g of dried seaweed powder mixed with 8 g of $NaClO_2$ (Bleaching agent) with 200 mL sodium acetate buffer (pH – 4.5) at 60 ºC for 3 h. After that, it was washed with deionized water till neutral by using centrifuge. Then, 240 mL of 0.5 M NaOH was added to neutral biomass and took it to oven for 60 ºC for overnight. Then, again it was washed with deionized water until neutrality. After that 480 mL of HCl (5%)

was added to this biomass and heat till boiling and allow it to room temperature for overnight and further it was washed with deionized water till it became neutral. The resultant water added cellulose was processed with ultra- sonication (40 second pulsing 70% amplitude for 20 min) treatment to break its cell wall. After that, it was dried (Xiang et al., 2016).

2.3 **Preparation of Reduced Graphene Oxide (rGO)- Zinc Oxide (ZnO) nanowire deposited seaweed cellulose based anodic paper supercapacitor**

rGO- ZnO nanowire deposited seaweed cellulose based paper supercapacitor was prepared by using single step hydrothermal method. In this method, add 0.2 gm $ZnCl_2$, 20 g Na_2CO_3 with 30 mL water and stir it for 1 hour. After that, 2.0 gm seaweed cellulose, 0.5 gm graphene oxide (GO) powder and 30 mL water was added to it and stir it to at room temperature for 1 hour. Then, it was transferred to 150 mL teflon lined autoclave (Hydrothermal reactor) and put in to oven at 130 ºC for 17 h (Chauhan et al., 2015). After that, it was cooled at room temperature for further process. Then, opened the teflon lined autoclave and decanted the liquid layer and vacuum filtration for solid residue by using nylon filter membrane. Then, simple press was used to prepare handmade nano seaweed cellulose paper supercapacitor. Further, it was dried at 50 ºC (Bhutiya et al., 2018).

2.4 Characterization

rGO-ZnO nanowire deposited seaweed cellulose based anodic paper supercapacitor was analyzed by using various instrumental techniques such as Fourier transform infrared spectra (FT-IR), Thermo gravimetric analysis (TGA), scanning electron microscope (FE-SEM), Tensile strength and X-ray diffraction (XRD). This prepared paper supercapacitor device was measured under Cyclic voltammetry (CV), Galvanostatic charge/discharge (GCD) and Electrochemical impedance spectroscopy (EIS).

Microscopy of collected marine seaweed was carried out by using a polarized microscope (AXIO Imager.A2m, Zeiss).

The FT-IR spectra was carried out by using FT-IR spectrophotometer (Perkin Elmer, Spectrum 2). The range was 400–4000 cm^{-1} and used ATR for mode of operation.

XRD was carried out on a D8 Discover X-diffractometer (Bruker) using Cu-Kα radiation at an accelerating voltage of 40 kV and current of 40 mA. The range of 2θ is from 10º to 80º. Crystallinity index (CrI %) of prepared paper supercapacitor was calculated by following Segal's equation (Xiang et al., 2016):

$$CrI = \frac{(I_{max} - I_{min})}{I_{min}} \cdot 100 \quad (1)$$

where, I_{max} is the maximum intensity of main peak and I_{min} is the minimum intensity at a 2θ angle close to 18º for cellulose I.

The surface morphology of seaweed cellulose, ZnO nanorowire deposited seaweed cellulose and rGO-ZnO seaweed cellulose nanocomposites based paper supercapacitor were characterized by using FE-

SEM (Ultra-55, *Zeiss).* For this process, samples were placed over carbon tape on a 1 cm diameter and supper coated with gold for prior for imaging. The image was taken 10.0 KV acceleration voltage, using lens detector.

TGA of paper supercapacitor was analyzed by thermo gravimetric analyzer (Perkin Elmer,4000) from room temperature to 800 ºC at a heating rate of 10 ºC min^{-1} under nitrogen atmosphere.

The tensile strength of rGO-ZnO seaweed cellulose paper supercapacitor was analyzed by using 0.25 mm × 12 mm strips. Test was performed in UTM, Shimadzu by using 100 N load cells with1 mm/min strain rate.

2.5 Electrochemical Setup and Measurement

The electrochemical measurement of ZnO nanowire-cellulose nanocomposites as well as rGO-ZnO nanowire deposited cellulose nanocomposites were assessed in a two-electrode assembly. The Cyclic Voltammetry (CV) has been performed over two electrode system under Galvanostat/Potentiostat (Autolab PGSTAT 302 N). It is the fundamental analysis in which current flowing through an electrochemical cell is measured as the voltage is cycled over a specified range. It is typically measured at fix rate (Kuzmenko et al., 2017). This two electrodes system was set up and it is optimized under Autolab Galvanostat/Potentiostat for Cyclic Voltammetry, Galvanostatic Charge discharge and Electro Impedance spectroscopy.

2.6 Fabrication of paper supercapacitor

The rGO-ZnO nanowire deposited seaweed cellulose nanocomposite was optimized as electrodes for supercapacitor application. It is asymmetric device with nickel foils to make cell set up for further testing An asymmetric supercapacitor was fabricated by sandwiching a piece of filter paper (Whatman paper, 125 mm, Cat No 1001 125) as a separator with one electrode of rGO-ZnO nanowire deposited seaweed cellulose sheet (1.5 cm X 2 cm X 0.005 cm, 80 mg) and second electrode was activated charcoal with Ni metal connection strips. The filter paper role was to make ionic transfer smoother between the two electrodes. The sodium chloride (3M) electrolyte was used. The electrodes were immersed in the sodium chloride solutions for 10 minutes. CV, GCD and EIS measurements of the supercapacitor were conducted on Autolab (PGSTAT 302N) instruments (Zhou et al., 2019).

3. Result And Discussion

Figure 1 (a) shows that the digital image (1.9x) of *Chaetomorpha antennina*. It shows that several filaments with pores which same as reported elsewhere so it proves that this algae is *Chaetomorpha antennina* (Bhutiya et al., 2018). The yield of cellulose from filamentous seaweed was 32% by using simple bleaching agent without any harsh treatment.

3.1 XRD Analysis

X-ray peak of algae nanofiborous cellulose shown in Fig. 2 (a). It gave peaks between 13º to 22º. Generally, *Chaetomorpha* species consists predominantly cellulose I specially, I_{α} cellulose. This types of XRD peaks in algae mainly shown in green filamentous algae such as *cladophora*, *Chaetomorpha* etc. These mainly two peaks at 15.0º and 17.2º, which are not more common in other cellulose such as plant based cellulose. These peaks due to the specific planner direction of filamentous algae cell wall (Siddhanta et al., 2011). Generally, this cellulose have triclinic structure whereas higher plant and cotton cellulose consists monoclinic structure (I_{β}), This is a major difference in the structure of algae cellulose and higher plant cellulose. The peak at 15.0º correlate to the α [100] and β [110] planes whereas peak at 17.2º correlate to α [010] and β [110] lattice plane. The peak at 23.0º corresponds to the α [110] and β [200] planes. The peak 15.0º correlate to α [110] and β [200] lattice planes (Xiang et al., 2016). Higher plant cellulose have not this type of XRD spectra so it have to convert I_{α} triclinic structure by using highly acidic treatment. Generally, cellulose I_{α} triclinic have lower moisture absorption capacity so it not easily brittle.

Figure 2 (b) show that the XRD peak of graphene oxide (GO) powder. The XRD peak at 2θ = 11.2°, which corresponds to the (002) it indicates that the graphene oxide was obtained by Hummer's method (Liu, et al., 2015). Here, the peak at 2θ = 43.04º, 45.0º and 73.96º are the peaks of blank aluminum plate which is used as holder in powder method XRD which we can minimize. Figure 2 (c) show the Xrd peak of rGO-ZnO nanowire deposited seaweed cellulose paper, which show that the peaks at 15.0º, 17.2º and 23.0º was alpha cellulose peak as above discussed whereas peaks showed at 2θ value of 31.2º (100), 34.1º (002), 36.1º (101), 48.1º (102), 57.0º (110), 63.2º (103), 66.9º (200), 68.2º (112), 69.1º (201) and 78.º1(004) with diffraction plane respectively. This all peaks were matched with JCPDS card no. 79–205 (Liewhiran et al., 2006 & Chauhan et al., 2015). Here, ZnO nanowires consists hexagonal wurtzite structure. The 2θ value at 26.02º is the weak diffraction peak which is for reduced graphene oxide (rGO) peak (Liu, et al., 2015), which clearly shows that it is amorphous in nature and also clearly proved that seaweed cellulose act as reducing agent because in Fig. 2 (b) that is the peak of graphene oxide powder (GO) and when this graphene oxide powder mixed with seaweed cellulose, it was reduced and gave Xrd peak of reduced graphene oxide (rGO) so no need to add sodium borohydride for reduction of GO which is mostly used in conventional method.

The Crystallinity index of rGO-ZnO deposited algae cellulose was 76.23% whereas extracted seaweed cellulose was 87.23% which also indicate that high degree of crystallinity due to presence of thick nanofibrils structure and it was proved that the heating and deposition process decreases the crystallinity of seaweed cellulose.

3.2 FTIR Analysis

Figure 3 (a) shows that the FTIR spectrum of graphene oxide powder. In this spectrum, the peaks around 3168 cm^{-1} and the lower intensity peaks at 1726 cm^{-1} due to the OH groups and stretching of -COOH

groups, respectively. The peaks nearby 1586 cm^{-1} due to sp^2 -hybridized carbon groups after oxidation. The peak at 1489 cm^{-1} due to graphite carbon as well as peak at 1398 cm^{-1} due to C-OH group which is in tertiary position. The peak at 1039 cm^{-1} due to alkoxy group in structure (Johra, et al., 2015).

In Fig. 3 (b) shows that the FTIR spectrum of rGO-ZnO-seaweed cellulose paper supercapacitor. In this spectra, peak at 3580 cm^{-1} mainly due to O-H stretching. The peak at 2998 cm^{-1} and 1271 cm^{-1} due to C-H vibration and bending O-H peaks. The peaks at 1130 cm^{-1} and 1022 cm^{-1} due to glycosidic bond of C-O-C and C-OH, respectively (Reddy et al., 2013). The peak at 569 cm^{-1} due to the Zn-O stretching vibration which was also same as reported elsewhere. In this FTIR spectra, the peak at 3580 cm^{-1} decreases intensity due to interaction of -OH group with zinc ion so it decreased -OH group in seaweed cellulose. This peak also revealed that the decomposition of carboxyl group in GO. The intense peak at 1439 cm^{-1} due to restoration of the sp^2 carbon which is confirmed peak of rGO (Gong et al., 2015).

3.3 Thermal stability

The thermo gravimetric analyses of ZnO-rGO seaweed cellulose paper and GO powder were showed in Fig. 4 (a) and (b), respectively. In Fig. 4 (a) showed that the weight loss started nearby 100 ^oC due to the vaporization of moisture adsorbed by cellulose paper. The major thermal degradation in ZnO-rGO seaweed cellulose paper was between 130 ^oC to 320 ^oC which was due to the degradation of algae cellulose. The maximum mass loss at this step was nearly about 30%. In the third stage, the weight loss occurred between 320 ^oC to 720 ^oC and this was due to the degradation of polymeric chains whereas above this temperature only carbonaceous residue was left. Here, the total weight loss of ZnO-rGO cellulose paper was 55% which showed that this composite have more thermal stability as compared to cellulose as reported elsewhere (Chauhan et al., 2015).

In Fig. 4 (b) showed thermal behavior of GO powder. It showed that the initially slight degradation occurred nearby 100 ^oC, this was due to the evaporation of water in GO powder whereas the major thermal degradation in GO powder was between 140 ^oC to 240 ^oC. This might be due to the chemical decomposition of oxygen based functional groups and major weight loss of GO powder between this temperature was nearly 40% (Kumar et al., 2019). The total weight loss of GO powder at 800 ^oC was 76%. Generally, GO is less stable as compare to rGO because rGO weight loss from 10 ^oC to 800 ^oC only 11%. This might be due to the vander waals force between the layer where oxygen functional groups removed (Cui et al., 2011).

3.4 SEM Analysis

Figure 5 (a) shows that the SEM image of nanofibrous seaweed cellulose sheet which clearly showed that the highly porous membrane was formed and each nanofibers twisted with each other to form spider's web type network. Generally, in all higher plants, the cellulose structure is different as compare to filamentous seaweed. This is due to different terminal complexes in structure because in higher plant, terminal complexes have rosettes six hexagonally structure with random orientation whereas filamentous

seaweed such as *cladophora* or *chaetomorpha* species have liner type of terminal complex with high degree of orientation so it have I_{α} type structure with naturally whereas, in higher plant it have I_{β} type structure which can also prove in XRD peaks as mentioned by Moon et al. This is the major difference between cellulose extracted from filamentous seaweed species and higher plants. Due to this difference, any harsh treatment such as enzymatic hydrolysis, mechanical treatment or acid hydrolysis is not require for extraction of nanofibrous cellulose from filamentous seaweed whereas, for extraction of cellulose from higher plant, this is required (Xiang et al., 2016). The average size of seaweed nanofibers from SEM image was 36 nm.

Figure 5 (b) shows that the SEM image of ZnO nanowire deposited seaweed cellulose sheet. It clearly, shows that nanowires were perfectly grown over seaweed nanofibrous network. ZnO nanowire were grown over *Ulva faciata* seaweed as reported in our previous work but this sheet was brittle due to I_{β} cellulose was in its cell wall (Bhutiya et al., 2018) whereas in present work, I_{α} cellulose which have also proved in XRD spectra of cellulose. It have also tensile strength as well as high yield (Gustafsson et al., 2016).

Generally, when seaweed cellulose was mixed with zinc chloride and sodium carbonate, the hydroxyl group over cellulose structure was interact with zinc ions to form zinc-cellulose complex and nucleation was formed over the cellulose surface during hydrothermal process. When the temperature and time increases, it formed nanowire from the nucleation on seaweed cellulose surface (Chauhan et al., 2015). Generally, size, structure and position of ZnO nanowire were depend on temperature and sodium carbonate concentration because lower concentration of zinc and sodium carbonate formed larger rods or wire type structure. Here, in Fig. 5 (b), clusters of nanorwires were formed in some places, this might be due to lower concentration of sodium carbonate because when increases the concentration, it became saturate and gave more ZnO nanowire with separately and also higher temperature also effect but in this present work, nearly about 200 ^{o}C, cellulose was start to degrade so it is better to do hydrothermal method at lower temperature (Kuzmenko et al., 2017).

In Fig. 5 (c-f) shows that rGO-ZnO nanowire deposited seaweed cellulose paper supercapacitor. The uniform layer of rGO (reduced graphene oxide) and ZnO nanowires clearly showed in SEM images. Generally, rGO which mainly consists polar oxygen containing groups as well as have an excellent vander waals force and strong hydrogen bonding so it can easily bind with seaweed cellulose (Magar et al., 2021).

3.5 Tensile test

Figure 6 showed that the tensile property of prepared rGO-ZnO seaweed cellulose paper supercapacitor. The tensile strength (σ_b) of this paper was 7.2 MPa as well as tensile module was 0.6 GPa. The maximum strain was 3.8%. This data showed that this paper supercapacitor have high tensile property. Generally, this tensile property may slightly vary because it depends on seaweed climatic condition or

when it grows but *Chaetomorpha antennina* seaweed grow over rocks which consists very high tensile strength by its nature (Mihranyan, 2011).

3.6 Cyclic Voltammetry

The specific capacitance value was identified from cyclic voltammetry (CV). The specific capacitance of the electrode was calculated from the area under the CV curves. The voltage range was − 1.0V to + 1.0V. The different scan rates were applied of 5,10,20,50,100 mV/s. The measurements were done in the twoelectrode configuration by assembling device. The asymmetrical supercapacitor device was fabricated. The CV curves in Fig. 7 (a) show rGO-ZnO nanowire deposited cellulose based device cyclic voltammetry result as determined from 5 mV/s scan rate curve. The value of specific capacitance was 2.5 F/g and energy density was 1.38 Wh/kg. Results indicated that the electrical double layer capacitive behavior (EDLC) was shown. The shape of CV curves at lower scan rate between 5 to 20 mV/s is moderately rectangular without any faradic peaks. At higher scan rates such as 50 or 100 mV/s, the rectangular shape of CV curve becomes slightly distorted due to increased resistance of electrolyte ion transportation.

Figure 7 (b) shows the performance of electrochemical measurement of ZnO-cellulose nanocomposite material assessed in a two-electrode assembly. The value of specific capacitance was 0.28 F/g and energy density is 0.076 Wh/kg. So, from the calculated values we can state that by integrating rGO in ZnO-cellulose nanocomposite, we can achieve better energy density as compared to ZnO-cellulose nanocomposite.

3.7 Galvanostatic Charging and Discharging (GCD)

Galvanostatic charging and discharging (GCD) measurements were used to calculate the energy density and power density of supercapacitor device with composite electrode material. Figure 8 (a) shows the dependence of capacitance retention on number of cycles, with applied current density 0.125 A/g. We have assembled two different devices using ZnO-cellulose nanocomposite and rGO-ZnO cellulose nanocomposite. The specific capacitance of ZnO-cellulose nanocomposite was 0.118 F/g while energy density was $6.6*10^{-4}$ Wh/kg (Fig. 8(b)). However, when we have added the reduced graphene oxide (rGO) in the same composition, the specific capacitance values and energy density have increased for rGO-ZnO cellulose device. The specific capacitance of rGO-ZnO cellulose nanocomposite was 37.5F/g while an energy density was 5.2 Wh/kg (Fig. 8 (c) for first ten cycles). It is proven from above calculation as compared to ZnO-cellulose nanocomposite that addition of rGO in an equal proportion of ZnO resulted in superior performance. Specific capacitance has improved by almost nine times and energy density has increased by almost eighteen times due to rGO. The rGO-ZnO cellulose nanocomposite supercapacitor device has been measured for cyclic stability till 5000 cycles (Fig. 8 (d) for last cycles of GCD measurements).

3.8 Electrochemical Impedance Spectroscopy

Electrochemical Impedance Spectroscopy (EIS) refers to the measurement of frequency dependent resistance to the current flow in an assembled device. EIS can identify diffusion limited reactions within the device. Here, we have tested two different composite materials through EIS technique. Figure 9 (a) shows the EIS measurement of rGO-ZnO cellulose nanocomposite deposited cellulose material. Figure 9 (b) shows the EIS measurement of ZnO-cellulose nanocomposite. The equivalent circuit-based model is fitted to experimental data which evaluate the individual circuit elements of supercapacitor device. In general, the model predicts value of series resistance (R_S), charge transfer resistance (R_{ct}), double layer capacitance at the interface of electrodes (C_{dl}) and Warburg resistance (Z_W) (Wan et al., 2017). For rGO-ZnO-cellulose nanocomposite device, the value of R_S was found to be 2.16Ω (Fig. 9 (c)) and for ZnO-cellulose nanocomposite device, the value of R_S was found to be 326Ω (Fig. 9 (d). A significant reduction in R_S in ZnO-cellulose nanocomposite as compared to rGO-ZnO cellulose nanocomposite is attributed to the addition of rGO and formation of an electrically conducting network, this assembled device can be use as energy storage device after adding reduced graphene oxide.

4 Conclusion

Nanofibreous cellulose ($I_α$) was extracted from seaweed green filamentous seaweed *Chaetomorpha antennina* and rGO and ZnO nanowire deposited over this seaweed cellulose for making paper supercapacitor. It have high specific high capacitance (37.5 F/g) and high energy density (5.21 Wh/kg). It have no air degradation after 5000 cycle. This marine seaweed cellulose based anode material helps in development of the thinnest paper supercapacitor which is light weight, biodegradable, high tensile strength and it have an promising application in smart electronic devices.

Declarations

Ethics approval and consent to participate

Not Applicable

Consent for publication

Not Applicable

Availability of data and materials

The data availability and materials were searched from reference materials which should be cited in manuscript

Competing interests

The authors declare that they have no competing interest

Funding

This work was carried out independently without any funding agencies

Authors' contributions

P.B., B.T., Z.H. were designed the experiment as well as wrote manuscript. R.K. and Y.S. were done supercapacitor device analysis. A.R. and P.R. were monitored the experiment.

Acknowledgement:

Dr. Priyank L. Bhutiya thanks to GERMI Director General Dr. Biswajit Roy for providing all facilities and continuous support as well as also acknowledge SRDC-PDEU for instrumental analyses. Mr. Bharat Odedara also acknowledged for support in collection of seaweed.

References

1. Abdah, M. A. A. M., Azman, N. H. N., Kulandaivalu, S., & Sulaiman, Y. (2020). Review of the use of transition-metal-oxide and conducting polymer-based fibres for high-performance supercapacitors. *Materials & Design*, *186*, 108199.
2. Bhutiya, P. L., Mahajan, M. S., Rasheed, M. A., Pandey, M., Hasan, S. Z., & Misra, N. (2018). Zinc oxide nanorod clusters deposited seaweed cellulose sheet for antimicrobial activity. *International journal of biological macromolecules*, *112*, 1264-1271.
3. Bhutiya, P. L., Misra, N., Rasheed, M. A., & Hasan, S. Z. (2018). Nested seaweed cellulose fiber deposited with cuprous oxide nanorods for antimicrobial activity. *International journal of biological macromolecules*, *117*, 435-444.
4. Bhutiya, P. L., Misra, N., Rasheed, M. A., & Hasan, S. Z. (2020). Silver Nanoparticles Deposited Algal Nanofibrous Cellulose Sheet for Antibacterial Activity. *BioNanoScience*, *10*(1), 23-33.
5. Chauhan, I., Aggrawal, S., & Mohanty, P. (2015). ZnO nanowire-immobilized paper matrices for visible light-induced antibacterial activity against Escherichia coli. *Environmental Science: Nano*, *2*(3), 273-279.
6. Cui, P., Lee, J., Hwang, E., & Lee, H. (2011). One-pot reduction of graphene oxide at subzero temperatures. *Chemical Communications*, *47*(45), 12370-12372.
7. Durairaj, A., Maruthapandi, M., Saravanan, A., Luong, J. H., & Gedanken, A. (2022). Cellulose Nanocrystals (CNC)-Based Functional Materials for Supercapacitor Applications. *Nanomaterials*, *12*(11), 1828.
8. Etana, B. B., Ramakrishnan, S., Dhakshnamoorthy, M., Saravanan, S., Ramamurthy, P. C., & Demissie, T. A. (2020). Functionalization of textile cotton fabric with reduced graphene oxide/MnO2/polyaniline based electrode for supercapacitor. *Materials Research Express*, *6*(12), 125708.

9. Gong, Y., Li, D., Fu, Q., & Pan, C. (2015). Influence of graphene microstructures on electrochemical performance for supercapacitors. *Progress in Natural Science: Materials International*, *25*(5), 379-385.
10. Gustafsson, S., Lordat, P., Hanrieder, T., Asper, M., Schaefer, O., & Mihranyan, A. (2016). Mille-feuille paper: A novel type of filter architecture for advanced virus separation applications. *Materials Horizons*, *3*(4), 320-327.
11. Hussain, S. Z., Ihrar, M., Hussain, S. B., Oh, W. C., & Ullah, K. (2020). A review on graphene based transition metal oxide composites and its application towards supercapacitor electrodes. *SN Applied Sciences*, *2*(4), 1-23.
12. Jiang, L., Han, S. O., Pirie, M., Kim, H. H., Seong, Y. H., Kim, H., & Foord, J. S. (2021). Seaweed biomass waste-derived carbon as an electrode material for supercapacitor. *Energy & Environment*, *32*(6), 1117-1129.
13. Johra, F. T., & Jung, W. G. (2015). Hydrothermally reduced graphene oxide as a supercapacitor. *Applied Surface Science*, *357*, 1911-1914.
14. Jose, J., Thomas, V., Vinod, V., Abraham, R., & Abraham, S. (2019). Nanocellulose based functional materials for supercapacitor applications. *Journal of Science: Advanced Materials and Devices*, *4*(3), 333-340.
15. Kumar, R., Singh, R., Gurjar, A., Kashyap, R., Kumar, M., & Kumar, D. (2019, August). Study the thermal stability of functionalized graphene oxide. In *AIP Conference Proceedings* (Vol. 2142, No. 1, p. 040015). AIP Publishing LLC.
16. Kuzmenko, V., Wang, N., Haque, M., Naboka, O., Flygare, M., Svensson, K., Gatenholm, P., Liu, J.& Enoksson, P. (2017). Cellulose-derived carbon nanofibers/graphene composite electrodes for powerful compact supercapacitors. *RSC advances*, *7*(73), 45968-45977.
17. Liewhiran, C., Seraphin, S. A., & Phanichphant, S. (2006). Synthesis of nano-sized ZnO powders by thermal decomposition of zinc acetate using Broussonetia papyrifera (L.) Vent pulp as a dispersant. *Current Applied Physics*, *6*(3), 499-502.
18. Liu, G., Wang, L., Wang, B., Gao, T., & Wang, D. (2015). A reduced graphene oxide modified metallic cobalt composite with superior electrochemical performance for supercapacitors. *RSC Advances*, *5*(78), 63553-63560.
19. Magar, H. S., Hassan, R. Y., & Mulchandani, A. (2021). Electrochemical impedance spectroscopy (EIS): Principles, construction, and biosensing applications. *Sensors*, *21*(19), 6578.
20. Mihranyan, A. (2011). Cellulose from cladophorales green algae: From environmental problem to high-tech composite materials. *Journal of Applied Polymer Science*, *119*(4), 2449-2460.
21. Missoum, K., Belgacem, M. N., & Bras, J. (2013). Nanofibrillated cellulose surface modification: a review. *Materials*, *6*(5), 1745-1766.
22. Moon, R. J., Martini, A., Nairn, J., Simonsen, J., & Youngblood, J. (2011). Cellulose nanomaterials review: structure, properties and nanocomposites. *Chemical Society Reviews*, *40*(7), 3941-3994

23. Reddy, K. O., Maheswari, C. U., & Shukla, M. (2013). Physico-chemical characterization of cellulose extracted from ficus leaves. *Journal of Biobased Materials and Bioenergy*, *7*(4), 496-499.
24. Rabani, I., Yoo, J., Bathula, C., Hussain, S., & Seo, Y. S. (2021). The role of uniformly distributed ZnO nanoparticles on cellulose nanofibers in flexible solid state symmetric supercapacitors. *Journal of Materials Chemistry A*, *9*(19), 11580-11594.
25. Saranya, M., Ramachandran, R., & Wang, F. (2016). Graphene-zinc oxide (G-ZnO) nanocomposite for electrochemical supercapacitor applications. *Journal of Science: Advanced Materials and Devices*, *1*(4), 454-460.
26. Siddhanta, A. K., Chhatbar, M. U., Mehta, G. K., Sanandiya, N. D., Kumar, S., Oza, M. D., Prasad, K. & Meena, R. (2011). The cellulose contents of Indian seaweeds. *Journal of applied phycology*, *23*(5), 919-923.
27. Sultana, F., Wahab, M. A., Nahiduzzaman, M., Mohiuddin, M., Iqbal, M. Z., Shakil, A., Mamun, A.A., Khan, M.S.R., Wong, L. & Asaduzzaman, M. (2022). Seaweed farming for food and nutritional security, climate change mitigation and adaptation, and women empowerment: A review. *Aquaculture and Fisheries*.
28. Wan, C., Jiao, Y., & Li, J. (2017). Flexible, highly conductive, and free-standing reduced graphene oxide/polypyrrole/cellulose hybrid papers for supercapacitor electrodes. *Journal of Materials Chemistry A*, *5*(8), 3819-3831.
29. Wang, K., Gao, S., Du, Z., Yuan, A., Lu, W., & Chen, L. (2016). MnO2-Carbon nanotube composite for high-areal-density supercapacitors with high rate performance. *Journal of Power Sources*, *305*, 30-36.
30. Wang, Z., Tammela, P., Strømme, M., & Nyholm, L. (2017). Cellulose-based supercapacitors: material and performance considerations. *Advanced Energy Materials*, *7*(18), 1700130.
31. Xiang, Z., Gao, W., Chen, L., Lan, W., Zhu, J. Y., & Runge, T. (2016). A comparison of cellulose nanofibrils produced from Cladophora glomerata algae and bleached eucalyptus pulp. *Cellulose*, *23*(1), 493-503.
32. Zhou, S., Kong, X., Zheng, B., Huo, F., Strømme, M., & Xu, C. (2019). Cellulose nanofiber@ conductive metal–organic frameworks for high-performance flexible supercapacitors. *Acs Nano*, *13*(8), 9578-9586.

Figures

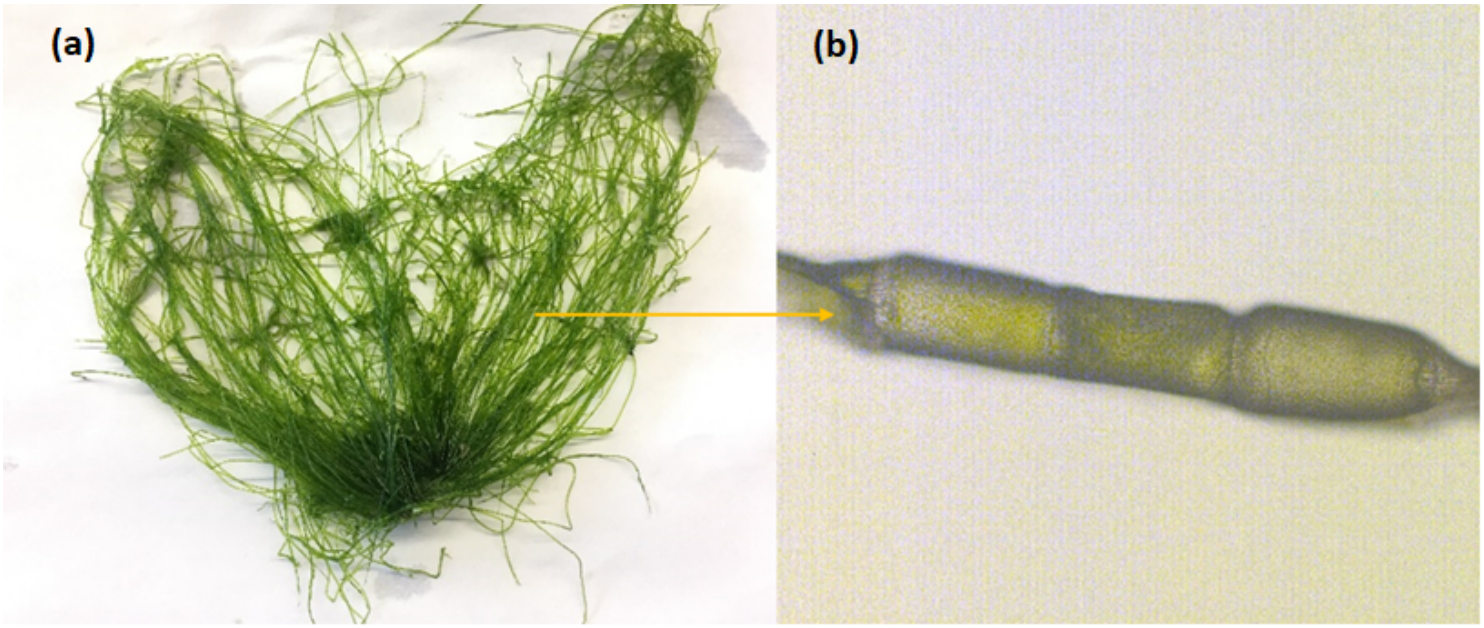

Figure 1

(a) Digital Photograph of *Chaetomorpha antennina* seaweed (b) Microscopic image of seaweed

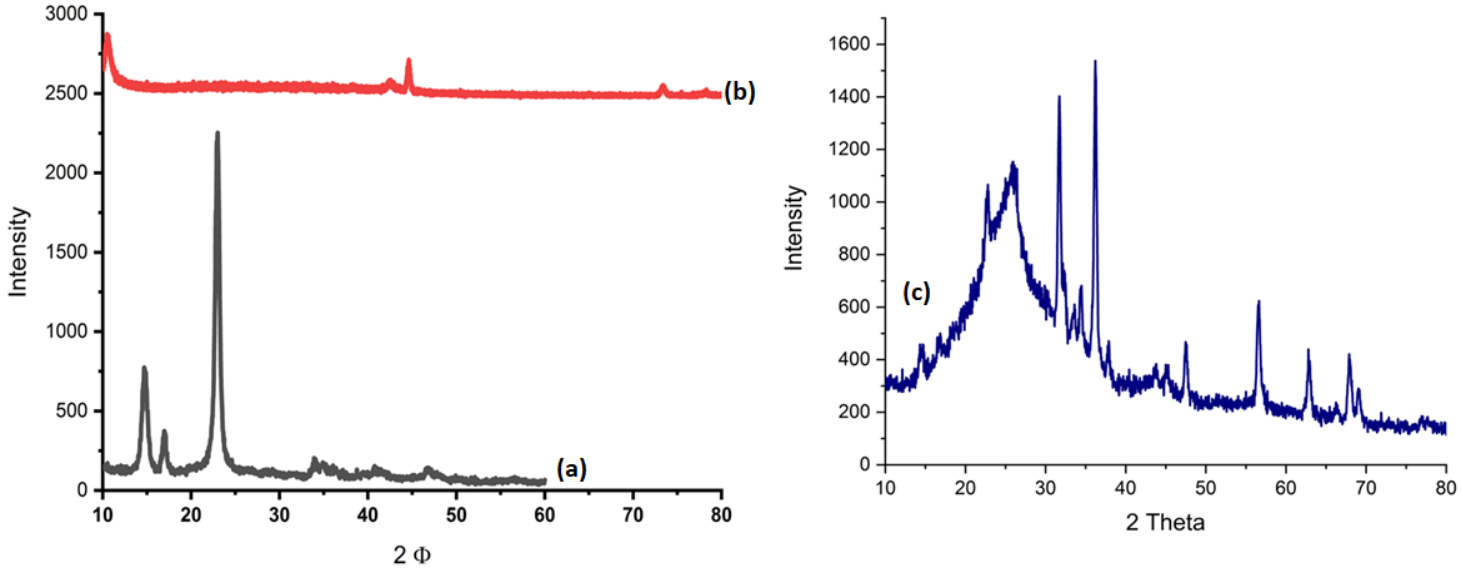

Figure 2

X-ray Diffraction Pattern of (a) Seaweed cellulose sheet (b) Graphene Oxide (GO) Powder (c) rGO- ZnO nanowire deposited seaweed cellulose paper supercapacitor

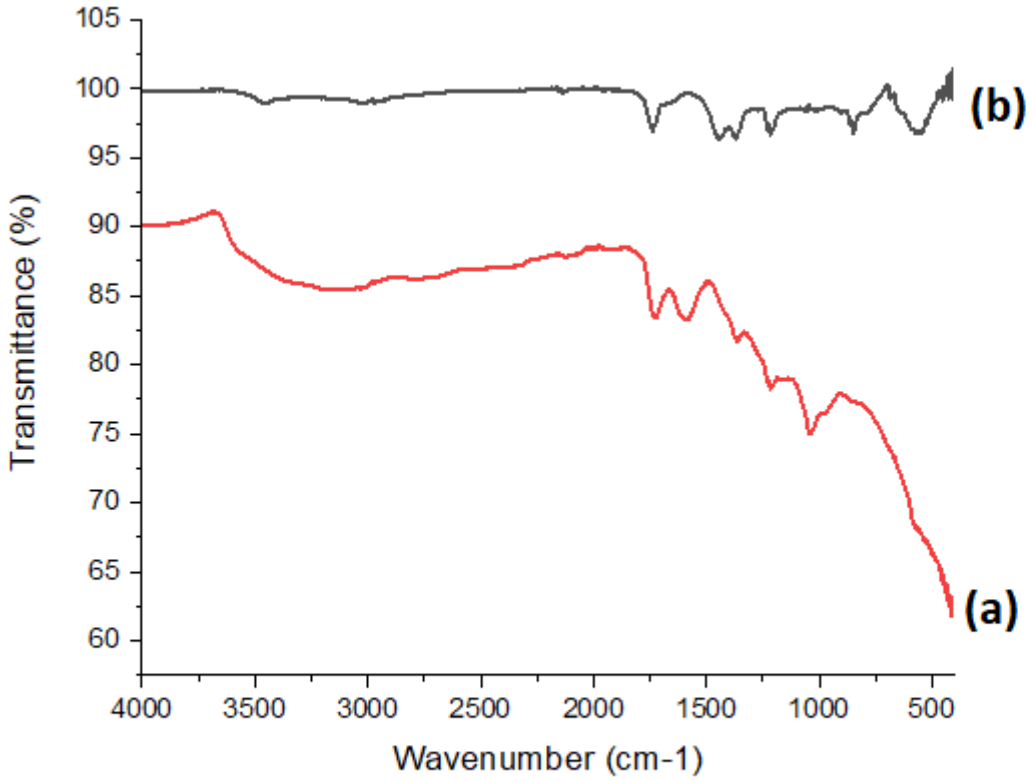

Figure 3

FT-IR spectrum of (a) Graphene Oxide (GO) Powder (b) rGO- ZnO nanowire deposited

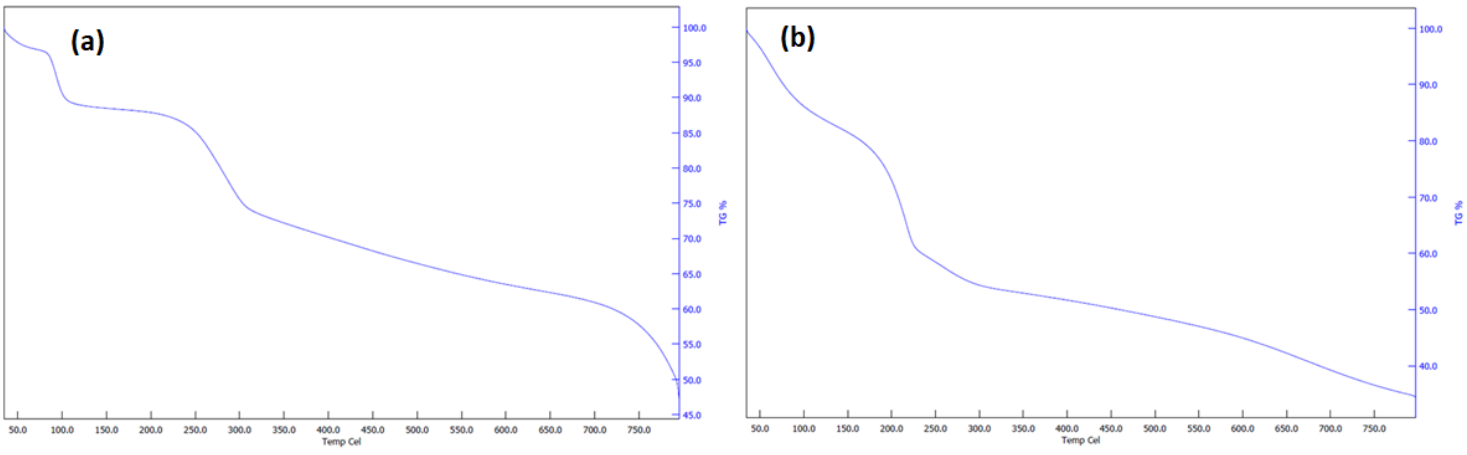

Figure 4

TGA analysis of (a) ZnO-rGO nanowire deposited seaweed cellulose paper supercapacitor (b) Graphene Oxide (GO) Powder

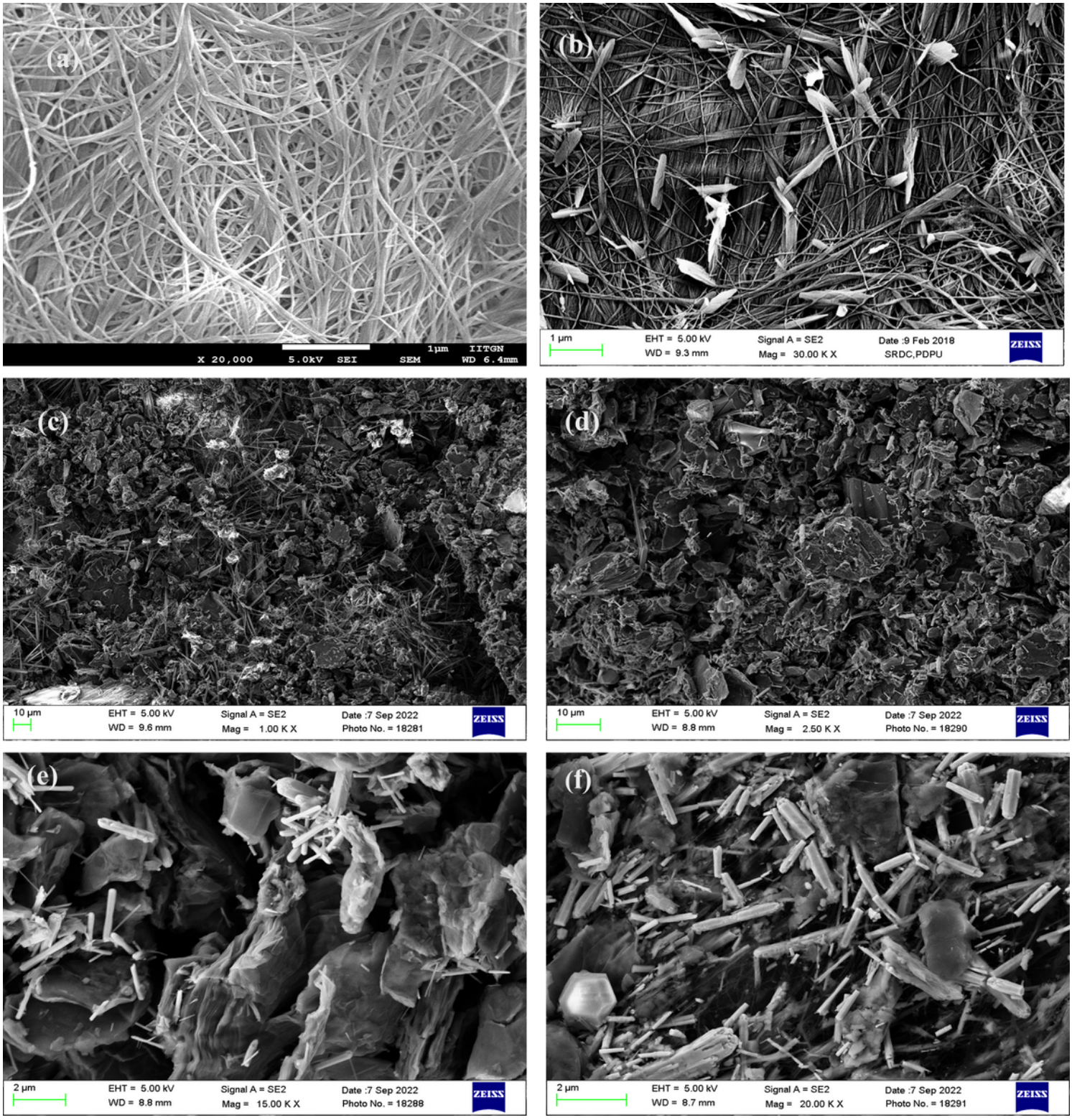

Figure 5

SEM image (a) Nanofibrous seaweed cellulose membrane (Spider's web network) (b) ZnO nanowire deposited seaweed cellulose sheet (c,d,e &f) rGO-ZnO nanowire deposited seaweed cellulose paper supercapacitor

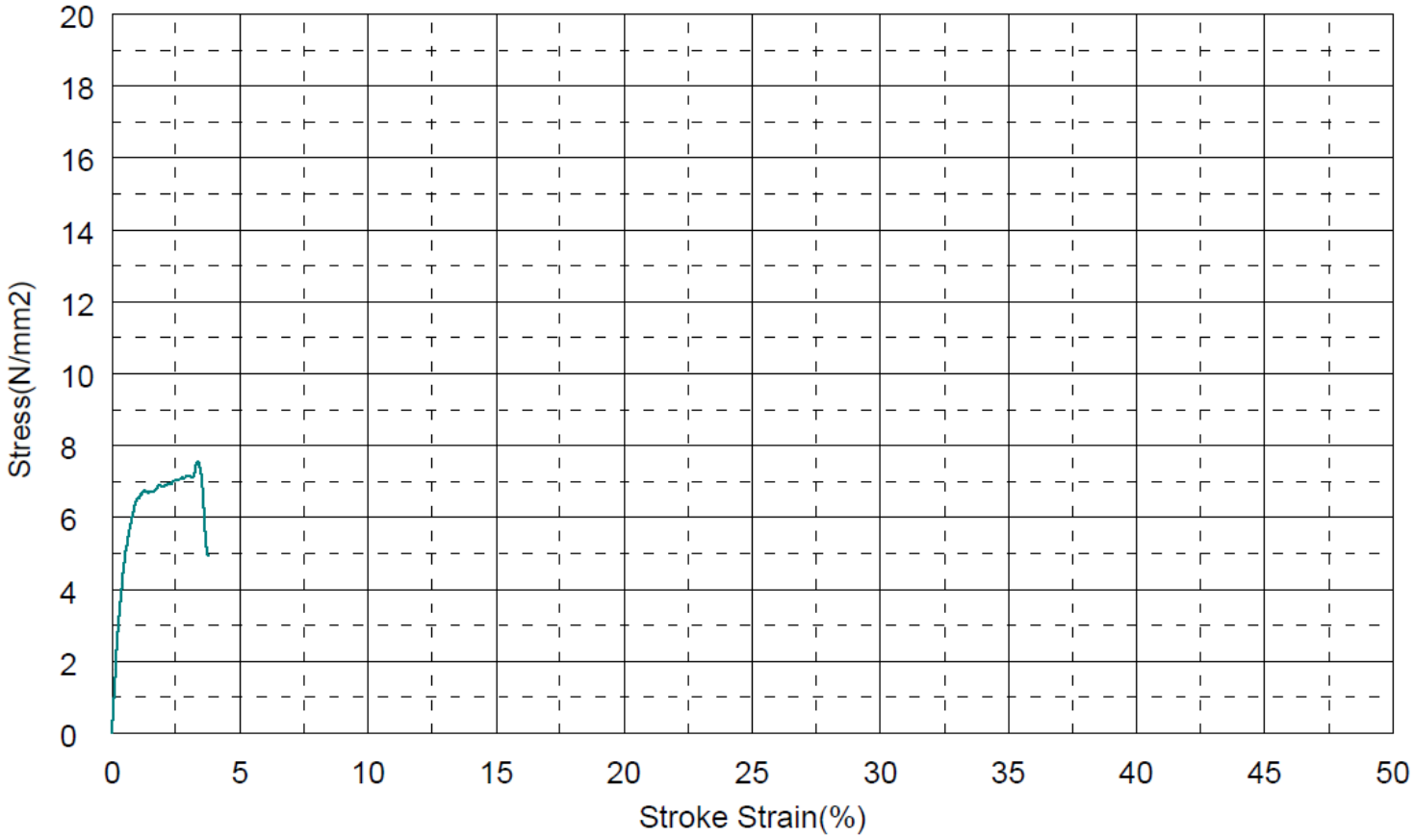

Figure 6

Tensile Strength of rGO-ZnO nanowire deposited seaweed cellulose sheet

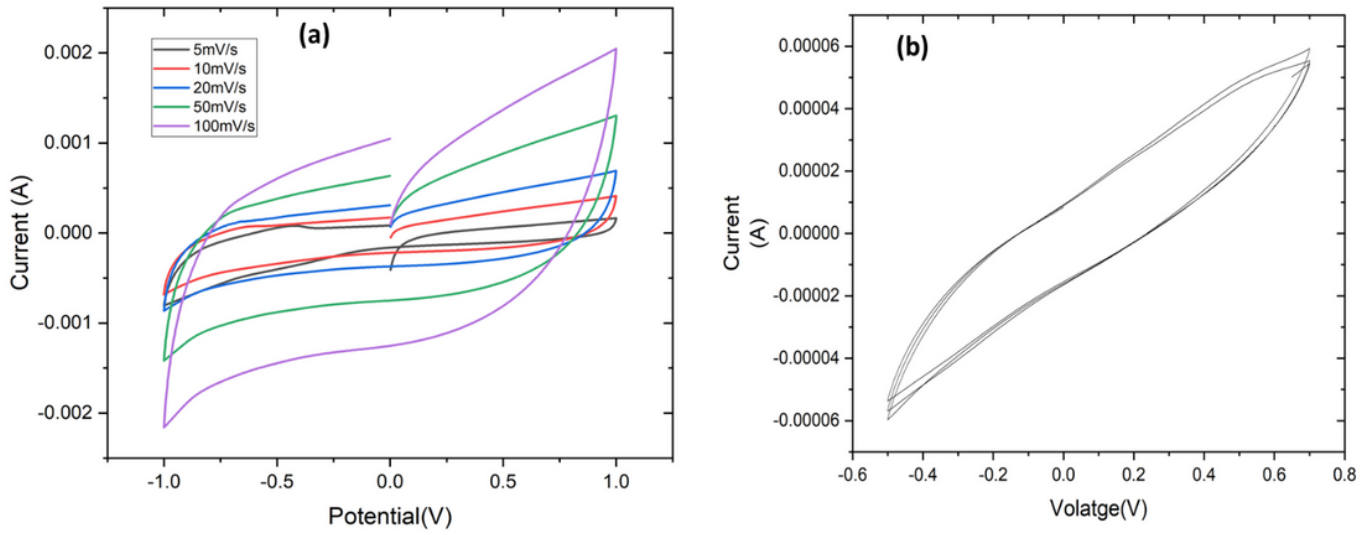

Figure 7

(a) Cyclic Voltammetry (Voltammogram) of rGO-ZnO cellulose nanocomposite

(b) Cyclic Voltammetry (Voltammogram) of ZnO cellulose nanocomposite

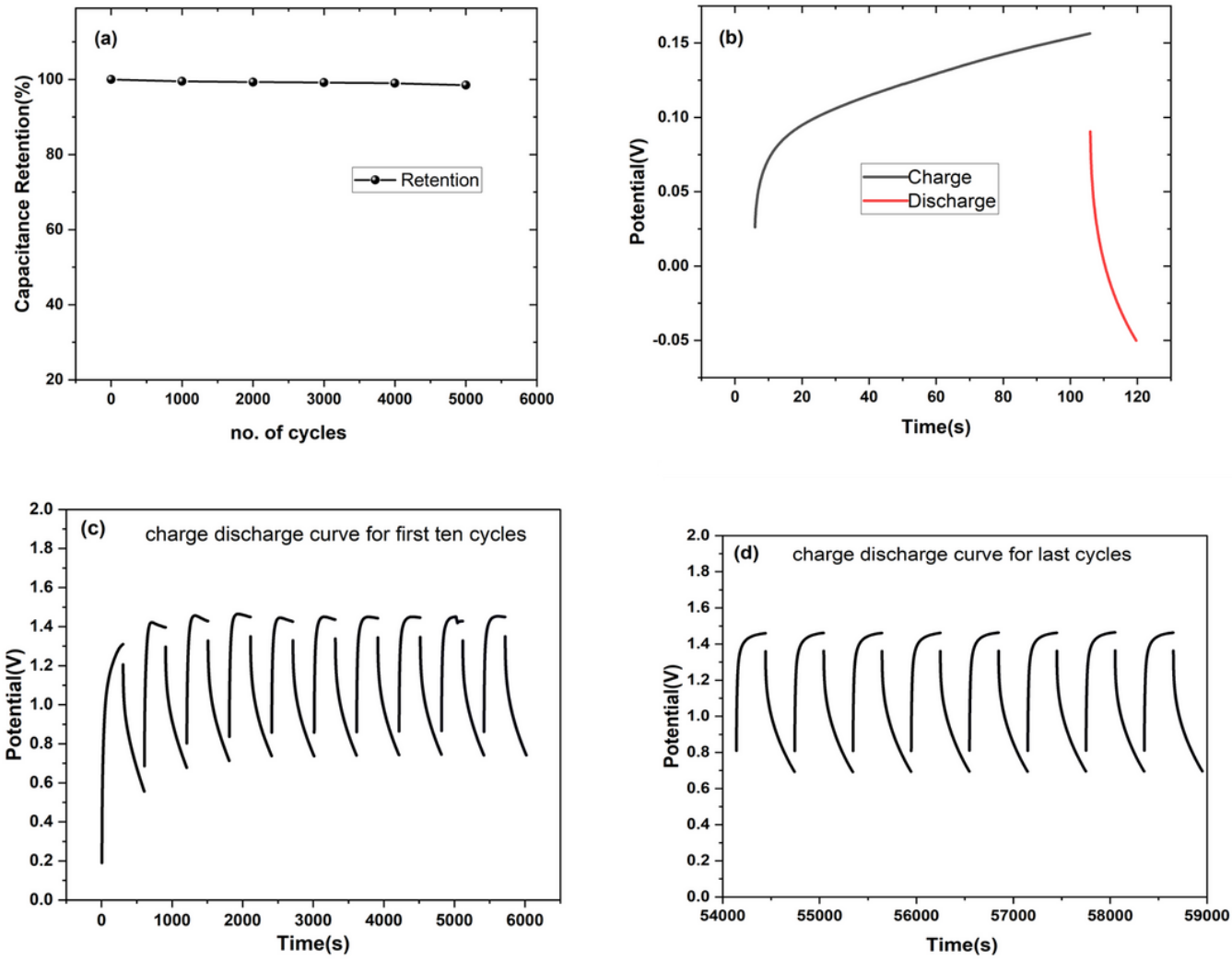

Figure 8

(a) GCD of rGO-ZnO cellulose nanocomposite (b) GCD of ZnO-cellulose nanocomposite (c) charge discharge curve for first 10 cycles of rGO-ZnO cellulose nanocomposites (d) charge discharge curve for last cycles of rGO-ZnO cellulose nanocomposites

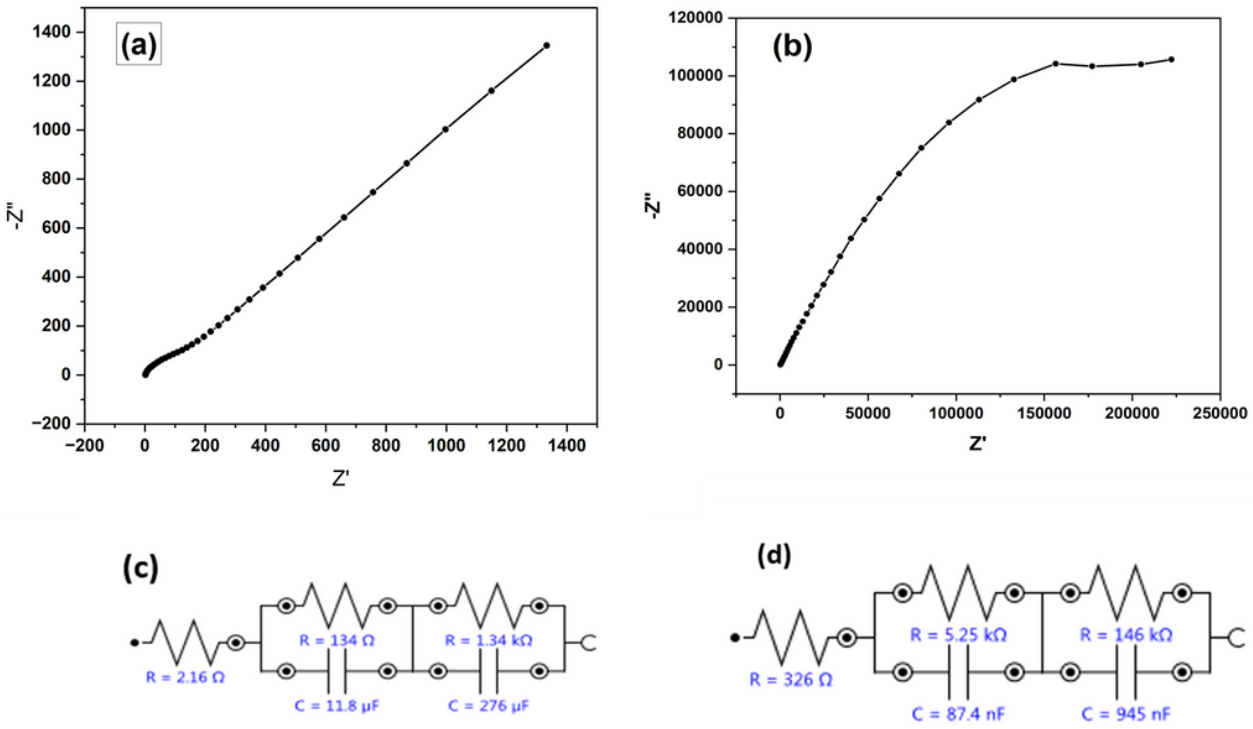

Figure 9

(a) EIS of of rGO-ZnO seaweed cellulose nano composite (b) EIS of ZnO-cellulose nanocomposite (c) equivalent circuit of rGO-ZnO-cellulose nanocomposite impedance spectrum (d) equivalent circuit of ZnO-cellulose nanocomposite impedance spectrum

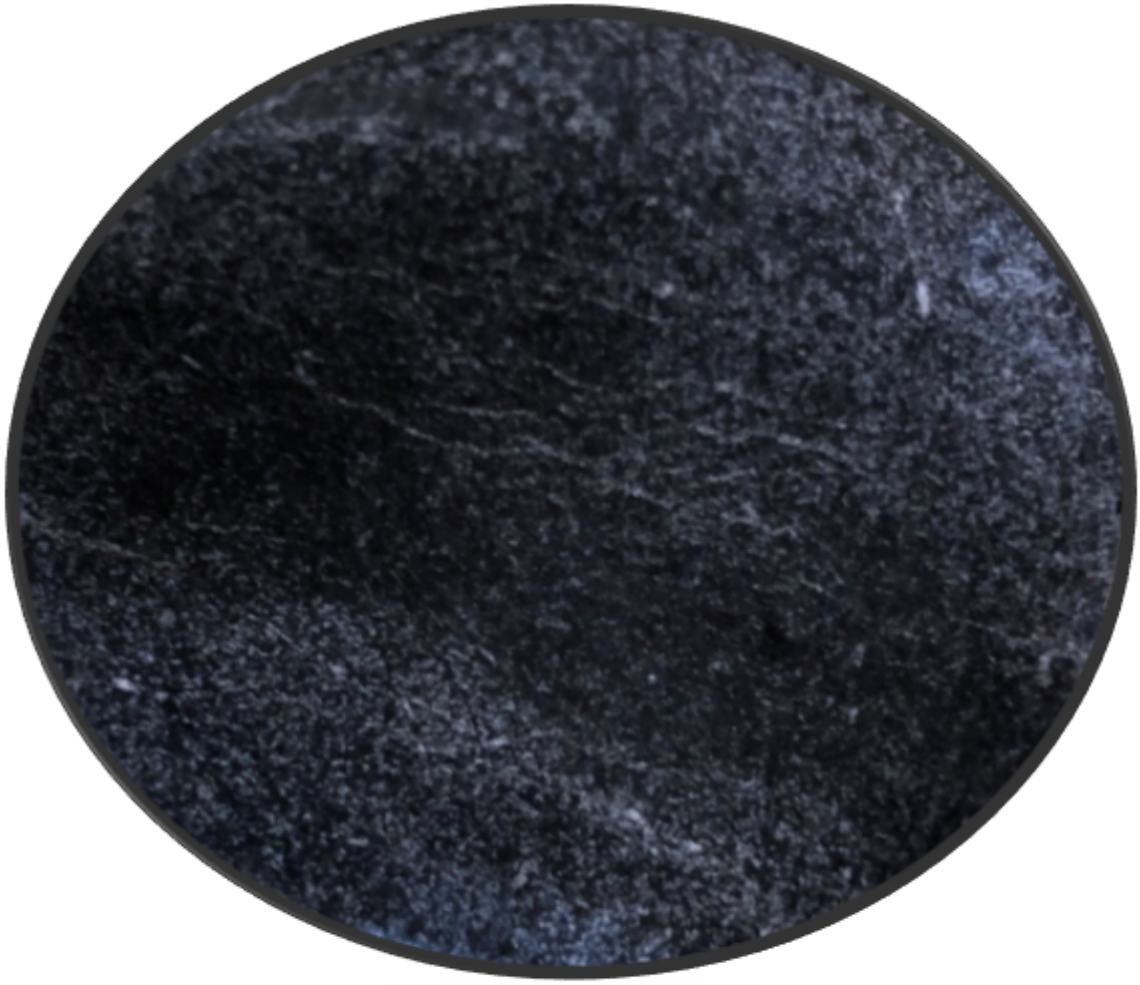

Figure 10

Digital image of rGO-ZnO deposited seaweed cellulose based paper supercapacitor

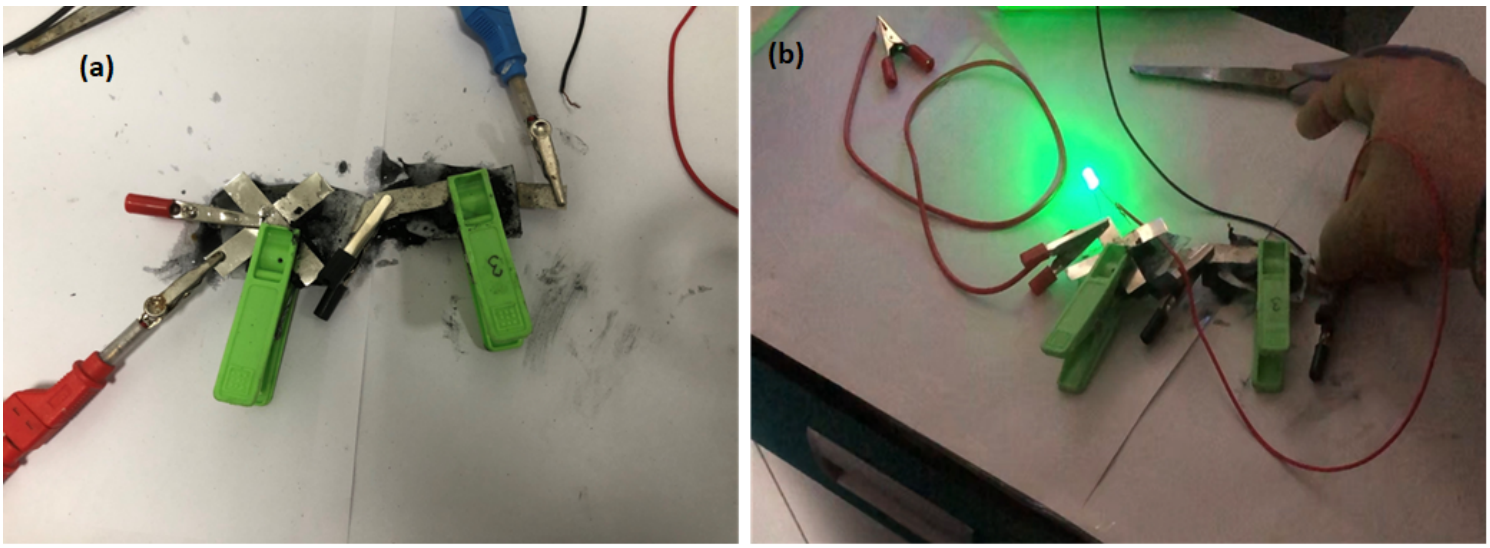

Figure 11

(a) ZnO-rGO seaweed cellulose anode paper supercapacitor and cathode charcoal device with Whatman filter paper separator (b) glow of LED (2.5 V) at this device

Supplementary Files

This is a list of supplementary files associated with this preprint. Click to download.

- GraphicalAbstract.png
- Supplymentoryinformation.pdf